Antigen-independent Activation Is Critical for the Durable Antitumor Effect of GUCY2C-targeted CAR-T Cells

Changsong Qi[1,#,*], Dongqun Liu[2,#], Chang Liu[3,#], Xiaofei Wei[2], Mingyang Ma[4], Xin-an Lu[2], Min Tao[4], Cheng Zhang[5], Xicheng Wang[4], Ting He[2], Jian Li[5], Fei Dai[2], Yanping Ding[2,*], Lin Shen[5,*]

[1]State Key Laboratory of Holistic Integrative Management of Gastrointestinal Cancers, Beijing Key Laboratory of Carcinogenesis and Translational Research, Department of Early Drug Development Centre, Peking University Cancer Hospital & Institute, Beijing 100142, China.

[2]Beijing Imunopharm Technology Co., Ltd., Beijing 100195, China

[3]Key Laboratory of Carcinogenesis and Translational Research (Ministry of Education/Beijing), Department of Early Drug Development Centre, Peking University Cancer Hospital & Institute, Beijing 100142, China

[4]Key Laboratory of Carcinogenesis and Translational Research (Ministry of Education/Beijing), Department of Gastrointestinal Oncology, Peking University Cancer Hospital & Institute, Beijing 100142, China

[5]State Key Laboratory of Holistic Integrative Management of Gastrointestinal Cancers, Beijing Key Laboratory of Carcinogenesis and Translational Research, Department of Gastrointestinal Oncology, Peking University Cancer Hospital & Institute, Beijing 100142, China

#These authors contributed equally.

*Corresponding authors:

Lin Shen, M.D., Email: shenlin@bjmu.edu.cn

Yanping Ding, Ph.D., E-mail: dingyanping@imunopharm.com

Changsong Qi, M.D., Email: changsongqi@bjmu.edu.cn

Qi C, *et al. J Immunother Cancer* 2024; 12:e009960. doi: 10.1136/jitc-2024-009960

Supplementary Methods

Plasmid construction and lentivirus production

The second-generation CAR molecules targeting GUCY2C was comprised of the signal peptide from colony stimulating factor 2 receptor alpha, a Strep tag II inserted into the N-terminal of scFv with (G4S) linker, different hinge regions derived from IgG4, CD8α, or CD28, transmembrane domains from CD8α or CD28, co-stimulatory domain from 4-1BB or CD28, and intracellular wildtype CD3ζ domain. The CAR genes were synthesized and inserted into the third-generation EF1α promoter-based lentiviral transfer plasmid pLenti6.3/V5 (ThermoFisher, Waltham, MA, USA). Lentivirus stock was prepared by transient transfection of a transfer plasmid, packaging plasmids (pLP1 and pLP2, ThermoFisher, Waltham, MA, USA) and an envelope plasmid (pLP/VSVG, ThermoFisher, Waltham, MA, USA) to HEK293T cells with using polyethyleneimine, collection of the culture medium 48h and 72h after transfection, ultrafiltration of the culture medium, and subsequent purification of the lentiviral particles using Core 700 chromatography (GE Healthcare, USA).

Short-time cytotoxicity assay

CAR-T cells were cocultured with target cells at different E:T ratios in X-VIVO. The target cells HCT-116-hGCC-H was stained with Calcein-AM (ThermoFisher, Cat#C3100MP) before coculture. After 5.5 hours, supernatants were collected and analyzed with the Varioskan™ LUX multimode microplate reader (ThermoFisher, VL0000D0).

Immunohistochemical staining

Human tissue microarrays (TMAs) were purchased from Bioaitech Company (Xi'an, China) and CDX tumor tissues were from the sacrificed tumor-bearing mice. About 3-4 μm thick tissue sections were deparaffinized, then subjected to antigen retrieval by boiling in 10 mM citric acid supplemented with 0.05% Tween-20 (pH 6.0) at 120°C for 10 min, subsequently quenched (by 0.3% H_2O_2; 15 min) and blocked with 10% goat serum in PBS (30 min) at room temperature. The primary antibody anti-GUCY2C (in house mouse IgG antibody) were incubated overnight at 2-8°C with 2 μg/mL, followed by the Anti-mouse IgG, HRP-linked Antibody (Cell Signaling, 7076S) for 30 minutes. Color was developed using eBioscience™ DAB chromogen for 5 minutes. After a rinse in water, Sections were subsequently counter-stained with Mayer's haematoxylin (Abcam, ab220365) and subjected to whole slide imaging (Olympus Optical Co Ltd, Japan).

Cytokine measurements

To determine cytokine production by CAR-T cells, cell supernatant was harvested 24 h after co-culture with HCT-116-hGCC-L cells. To measure cytokines levels, we used Cytokine Bead Array (CBA) Kit (BD Biosciences; Human IFN-γ Flex Set, Cat#560111; Human TNF Flex Set, Cat# 558273; Human IL-2 Flex Set, Cat# 558273; Human Soluble Protein CBA Buffer Kit, Cat#558264) according to manufacturer protocol. In brief, capture beads (IL-2, TNF and IFN-γ) and cell supernatant were co-incubated for 1 h. Then PE-detection reagents were incubated with the beads for another 2 h. Beads were washed and analyzed by ACEA Flow Cytometer (ACEA Biosciences, NovoCyte 2060R).

Tumor organoids culturing

The tumor tissue was immediately immersed in transfer media at 4°C post-dissection. After thorough washing with irrigation buffer (KS100121, Daxiang Biotech) until clarity was achieved, the cleaned tissue was finely minced and combined with dissociation reagent (KS100123, Daxiang Biotech). The solution was gently agitated for 30 min at 37°C. Subsequent to digestion, cells were harvested, suspended in rinsing buffer (KC100141, Daxiang Biotech), and filtered through a 100 μm cell strainer to eliminate undigested tissue debris. The resulting filtrate underwent centrifugation to collect cells, which were then resuspended in a mixture of culture medium (OC100131, Daxiang Biotech) and 3D matrigel (DatrixGel, Daxiang Biotech). This cell suspension was seeded into a 24-well plate for subsequent organoid culture. Regular medium changes every other day were instituted, and organoids were passaged every 7 days.

Supplementary Figures

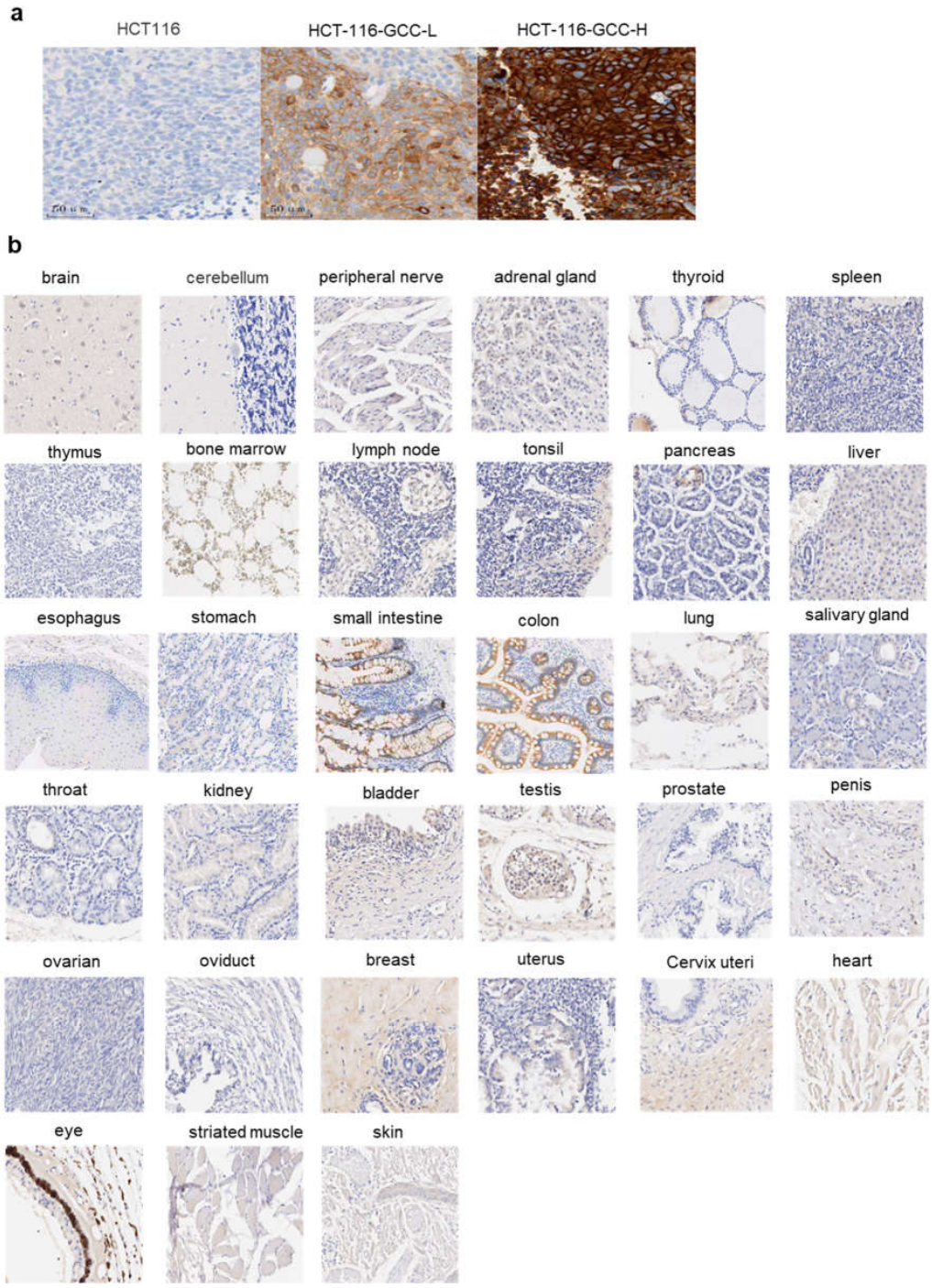

Figure S1. The GUCY2C expression in different tumor cell derived tumor tissues and in human normal tissues. (a) The expression of GUCY2C in HCT116, HCT-116-hGCC-L, and HCT-116-hGCC-H tumor tissues was analyzed using immunohistochemistry assay. The GUCY2C-targeted

antibody was developed by immunization of mice with the extracellular domain of GUCY2C and subsequent screening. HCT116, HCT-116-hGCC-L, and HCT-116-hGCC-H tumor tissue section was prepared using the xenograft tumors in nude mice. (b) IHC examination of GUCY2C expression in various normal tissues. This tissue microarray includes 33 types of normal tissues and organs.

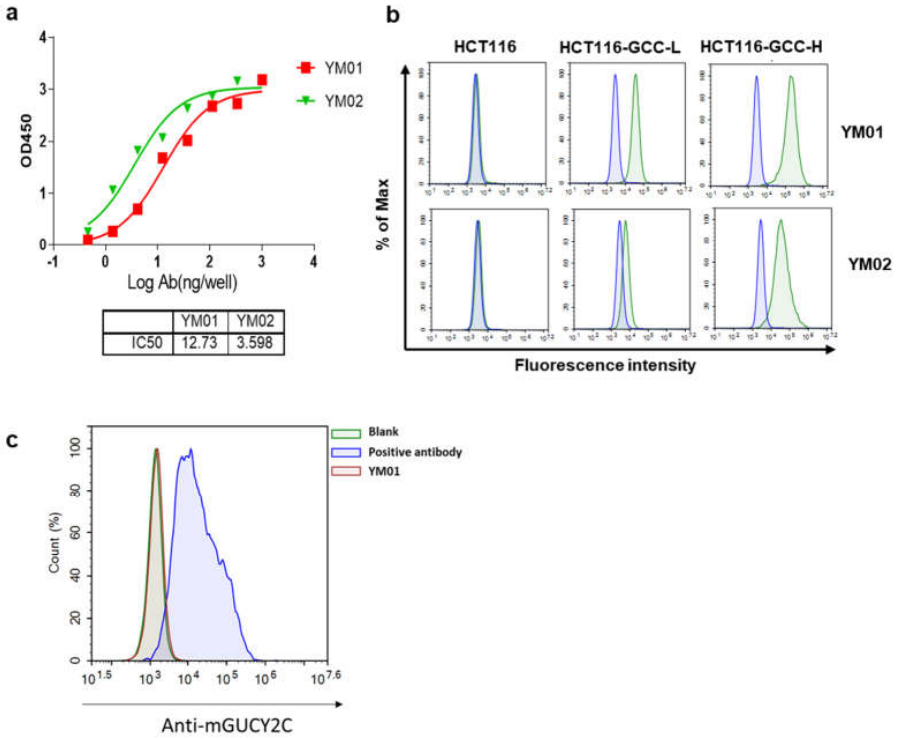

Figure S2. The binding efficiency of YM01 and YM02 to GUCY2C. (a) The ELISA assay showing the binding of YM01 and YM02 to the His-tagged human GUCY2C extracellular domain recombinant protein ($hGUCY2C_{ECD}$). YM01 and YM02 antibody were coated on the 96-well plate at different dilution concentrations, and then incubated with the $hGUCY2C_{ECD}$ protein for detection. (b) The flow cytometry assay showing the binding of YM01 and YM02 to HCT-116 cells with different GUCY2C expression. HCT116-hGCC-L, sorted cell clones with low density of GUCY2C expression; HCT116-hGCC-H, sorted cell clones with high density of GUCY2C expression. (c) The binding of YM01 to HEK293T cells overexpressing murine GUCY2C was analyzed by flow cytometry. Positive antibody, a commercial antibody targeting murine GUCY2C.

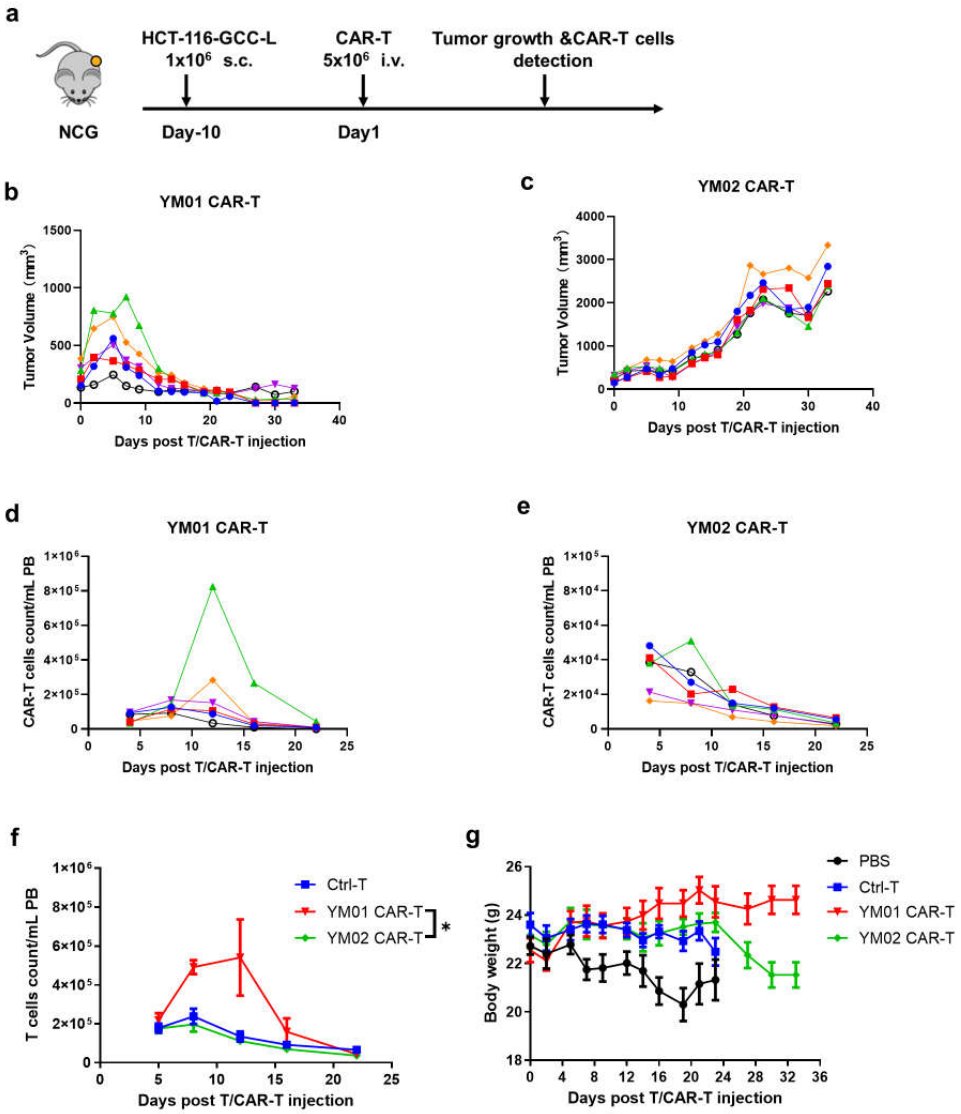

Figure S3. The antitumor effects and expansion of YM01 CAR-T and YM02 CAR-T in tumor-bearing mice. (a) Schema of the animal study design. NCG mice were inoculated subcutaneously with 1×10^6 of HCT-116-hGCC-L cells and received 5 million CAR-T cells per mouse intravenously 10 days later. (b-c) Individual tumor growth kinetics after YM01 CAR-T (b) or YM02 CAR-T (c) treatment (n=6). (d-e) Individual CAR-T expansion kinetics after YM01 CAR-T (d) or YM02 CAR-T (e) treatment (n=6). (f) The average number of $CD3^+$ T cells in the peripheral blood of mice in each group over time after treatment (n=6). (g) The average mouse body weight in each group over time after treatment (n=6).

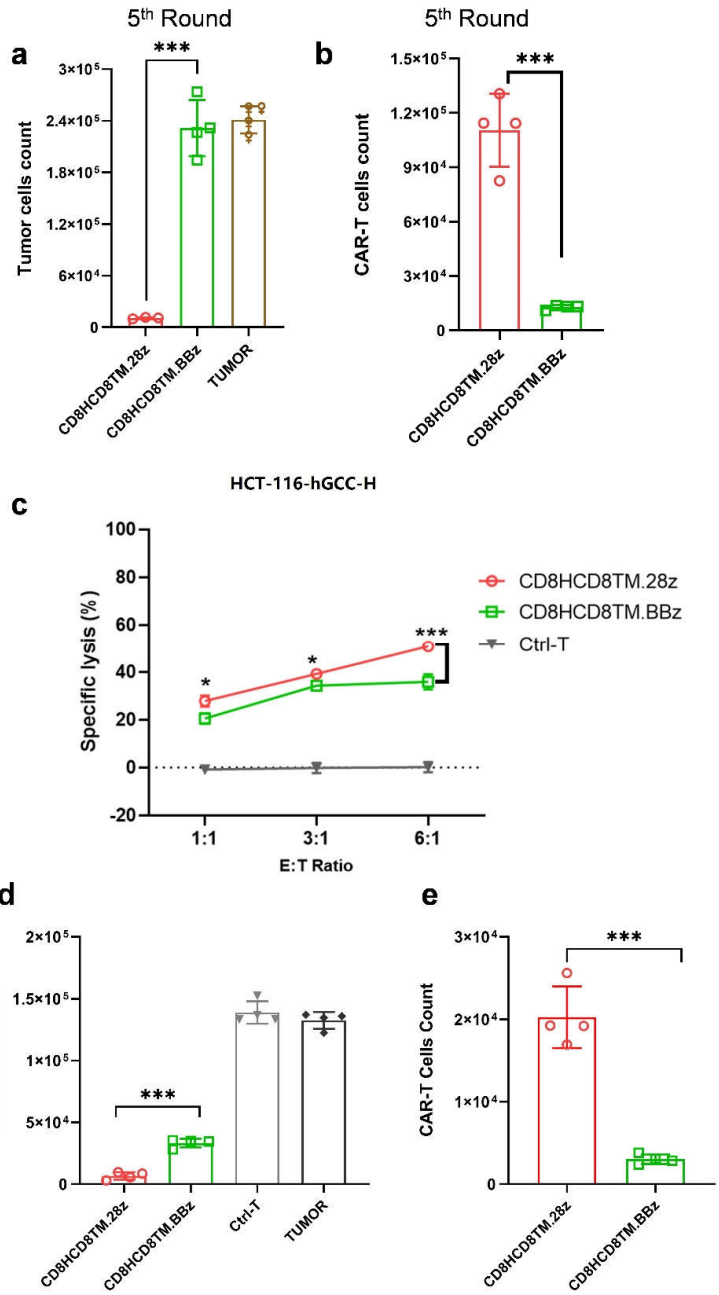

Figure S4. The effects of 28z and BBz CAR-T cells on HCT116-hGCC-L and HCT116-hGCC-H tumor cells in vitro. (a-b) The residual amount of tumor cells (a) and CAR-T cells (b) after chronic stimulation of HCT116-hGCC-L tumor cells for 5 times at the E:T ratio of 1:3. (c) Acute killing efficiency of HCT116-hGCC-H tumor cells by 28z and BBz CAR-T cells. CAR-T cells were co-cultured with HCT116-hGCC-H tumor cells at various E:T ratio for 4 h. (d-e) The residual amount of tumor cells and CAR-T cells after chronic stimulation of HCT116-hGCC-H tumor cells for 3 times at the E:T ratio of 1:1.

a

Hinge	Amino acid	Sequence
CD8H	45	TTTTPAPRPPTPAPTIASQPLSLRPEACRPAAGGAVHTR GLDFACD
CD28H	39	IEVMYPPPYLDNEKSNGTIIHVKGKHLCPSPLFPGPSKP
IgG4H	12	ESKYGPPCPPCP

TM	Amino acid	Sequence
CD8TM	24	IYIWAPLAGTCGVLLLSLVITLYC
CD28TM	27	FWVLVVVGGVLACYSLLVTVAFIIFWV

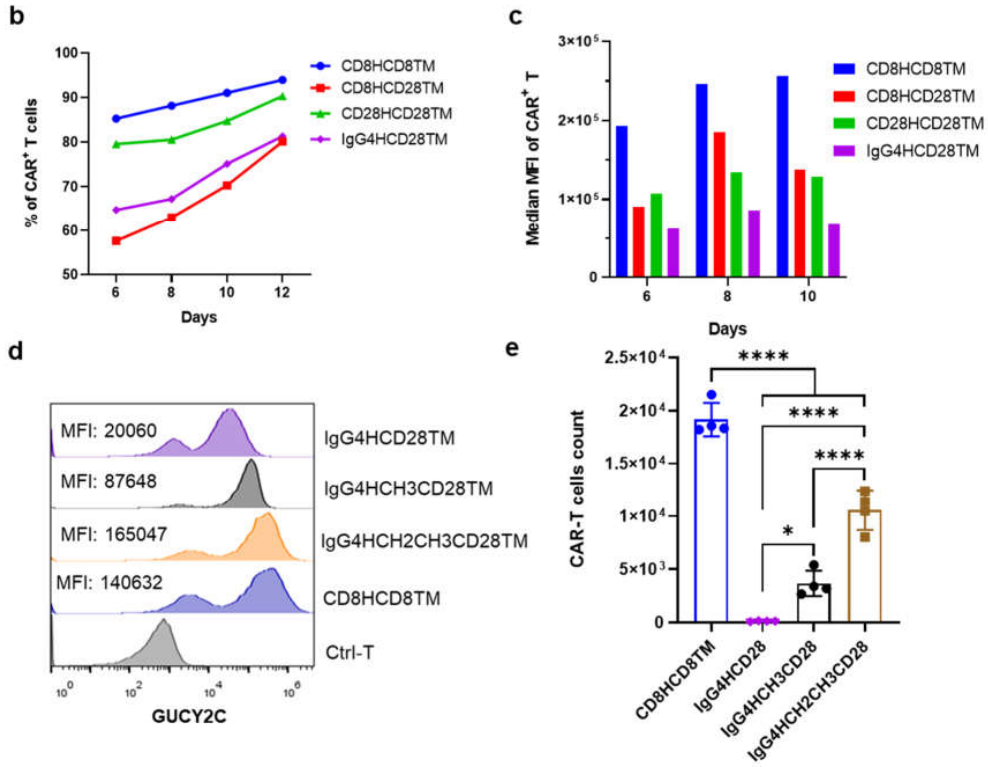

Figure S5. The effects of different hinge and transmembrane domains on the CAR expression, antigen binding, and antigen-stimulated expansion of YM01 CAR-T cells. (a) The amino Acid sequences of different hinge (CD8H, CD28H and IgG4H) and transmembrane (CD8TM and CD28TM) domains. The cysteine residues in each domain were marked in red. (b) The transduction efficiencies of YM01 CAR-T cells with different hinge and transmembrane domains were evaluated using flow cytometry. (c) The mean fluorescence intensity of YM01 CAR proteins in each CAR-T cell was evaluated using flow cytometry. (d) The quantity of hGUCY2C$_{ECD}$ protein binding to YM01 CAR-T cells with different hinge and transmembrane domains were evaluated using flow cytometry. (e) The amounts of residual CAR-T cells after repetitive stimulation with HCT-116-hGCC-L cells for three times.

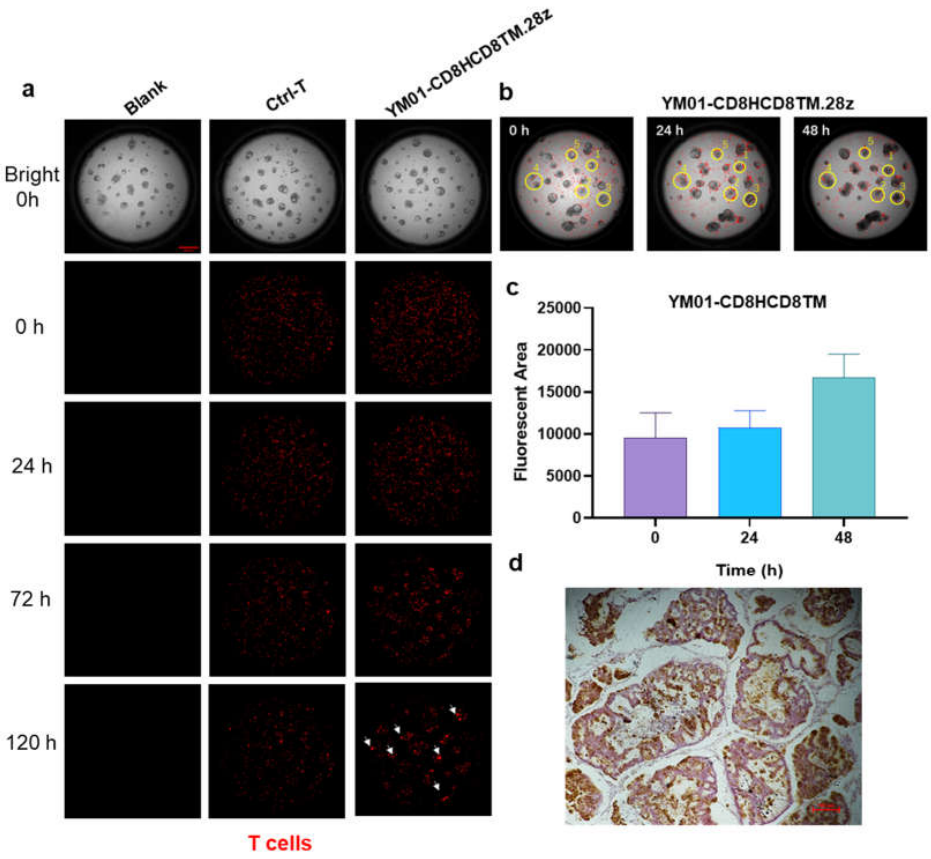

Figure S6 YM01-CD8HCD8TM.CD28z CAR-T cells exhibit strong infiltration ability in CRC organoids. (a) Representative brightfields and fluorescence images after co-culture of CRC organoids and YM01-CD8HCD8TM.CD28z CAR-T at the E:T ratio of 1:3 over time. T cells or CAR-T cells were labeled with cytotracker red. (b) Representative merged images showing the migration ability of YM01-CD8HCD8TM.CD28z CAR-T cells to organoids. (c) The fluorescence area of T cells surrounding the CRC organoids after co-culture over time in each group. (d) Immunohistochemistry staining showed the expression of GUCY2C in the CRC patient-derived xenograft (PDX) tumor tissue. Scale bar, 100 μm.

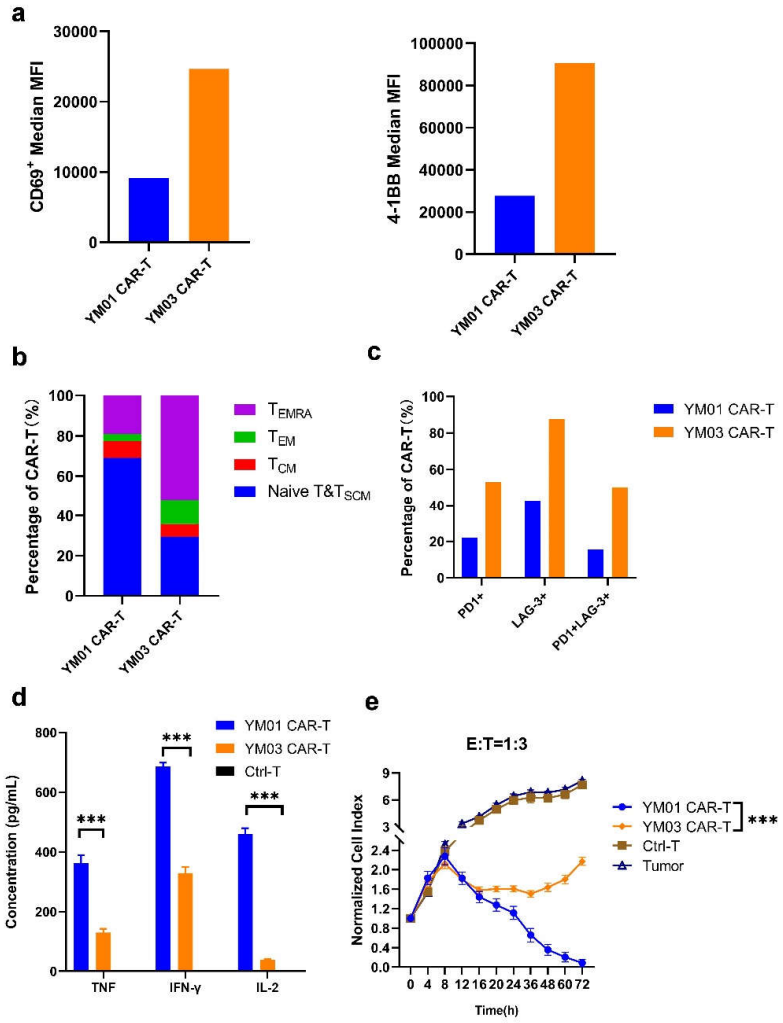

Figure S7. Comparison of the tonic signaling and antitumor activities of YM01 CAR-T and YM03 CAR-T cells. (a) The mean fluorescence intensities of CD69 and 4-1BB on the surface of CAR-T cells without antigen stimulation. (b) The proportions of various T cell subsets in CAR-T cells without antigen stimulation, including effector T cells (T_{EFF}), effector memory T cells (T_{EM}), central memory T cells (T_{CM}), and naïve and stem cell memory T cells (T_{SCM}). The T cell subsets were analyzed using flow cytometry labeling of CD62L and CD45RA. (c) The proportions of $PD1^+$, $LAG3^+$, and $PD1^+LAG3^+$ CAR-T cells in YM01 CAR-T and YM03 CAR-T groups. (d) The level of secreted cytokines of YM01 CAR-T and YM03 CAR-T after co-culture with HCT-116-hGCC-L cells for 24 h at the E:T ratio of 1:3. (e) Realtime cytotoxicity assay of YM01 CAR-T and YM03 CAR-T against HCT-116-hGCC-L cells at the E:T ratio of 1:3.